

Flexural Analysis of a Plate-type lying on Subgrade at a Constant Speed

Ogunyebi Segun Nathaniel, *Member, IAENG*

Abstract— An analytical technique for the solution of plate-type structural members due to the influence of torsional rigidity and other vital parameters is developed in this present study. The governing equation is addressed by the versatile method of Shadnam et al. The method specifically makes a reduction to the model equation. A parametric study that examined the dynamic influence of torsional rigidity, rotatory inertia, and variable elastic foundation on the plate flexure is carried out. It is found that these parameters greatly influenced the deflecting members (plate-type). Thus, a rise in the values of these structural parameters produces a noticeable effect on the critical (fundamental) velocity of the plate-type member. Hence, the hazard of a resonating effect is amply decreased.

Index Terms— Moving load, rectangular plate, elastic subgrade, effective torsional rigidity, distributed load.

I. INTRODUCTION

MOVING loads are forces acting on a structure and continually changing its position. The usefulness of the study in engineering designs and the transportation industry has attracted many authors. Common cases of members exhibiting flexures for loads that move (uniformly & non-uniformly) include tunnels, cableways, e.t.c. and these structures may be elastic, viscoelastic, or inelastic. The dynamic influence of loads resting on elastic structures attracted the attention of researchers in this area around the mid-nineteen century because of the effect of an increase in traffic intensity and speed.

Fryba [1] presented an exhaustive assessment of the subject of structural flexures for loads that move at speed (constant or variable). Loads (moving ones) on bodies are in two folds, one part is MF (moving force) where the consequence of inertia on the loads is assumed trivial and only the influence of force is to be considered. Observations from this assumption show that considerable errors arise from this. Thus, if inertia influence is taken into consideration, one is termed MM (moving mass). Oni [2] considered the dynamic vibrations of structural members when loads (moving one) and mass (for the structure) are compared in magnitude.

Moving loads on elastic structures for point-like has received significant attention from researchers. Milormir et al. [3] formulated a theory describing the Bernoulli-Euler beams behaviour as having concentrated moving masses. They used

the method of Fourier for the simply supported structure. Ogunyebi et al [4] considered the procedural vibrations of structures (no-uniform) and hence, a perfect deduction for the members by a numerical procedures. Al-Ansari and Afzal [5] developed a simple procedure to obtain deflection of uniform plate (regular & irregular) with concentrated loading system. Fedoseyer and Yagnyatinskiy [6] obtained solutions in analytical form for plate model affected by elastic actuators defined according to Hooke's law using integral transform methods. Gebre et al [7] investigated the influences of warping on beams (thin-walled) having restrained torsion for different types of sections.

Ogunyebi [8] presented procedures for the HMMDL lying on subgrade. Numerically, the rise in B-E model parameters gives a decrease in the magnitude.

However, for more reliable practical engineering designs, moving load on structural members is usually presented as a 'distributed' load instead of a 'concentrated' load. Therefore, for a detailed analysis of the deflection of structural members for acceptable accuracy, it is advisable to consider the beam or plate subjected to moving distributed load. Some authors made a tremendous effort in addressing this aspect of the study [9-10]. Oni and Ogunyebi [11] investigated the action of a uniform one-dimensional structure lying on a constant elastic subgrade with uniformly distributed weight by the method of generalized integral transform. Oni and Ogunyebi [12] presented a classical assessment of the problem of flexural response to one-dimensional members with distributed loading system.

Recently, Gao et al [13] analyzed the impact of ratios of aspect & Poisson on flexural motions of a plate (rectangular) with bc's and the results were validated by FEM. Sorrentino and Catania [14] considered the flexural behavior of a simply-supported Kirchhoff structure employing the method of Rayleigh-Ritz.

Interestingly, the influence of torsional rigidity & other vital parameters in the deflection of the two-dimensional system is highly essential and should not be jettisoned in structural design. The authors above failed to address this very important aspect. Thus, this present paper presents the flexural vibration of plate-type lying on variable elastic subgrade traversed by moving loads. Effects of the torsional rigidity, subgrade foundation modulus, and rotatory inertia on the structural vibration of the structure are examined.

II. PLATE-TYPE MOTION EQUATION

Motion equation for the plate-type deflection with torsional rigidity T_r (Alisjahbana et al., [15] and resting on an elastic foundation on variable elastic subgrade is

Manuscript received June 29, 2021; revised July 15, 2023.

Ogunyebi Segun Nathaniel is an Associate Professor at the Department of Mathematics, Ekiti State University, Ado Ekiti, 360001, Nigeria, (E-mail: segun.ogunyebi@eksu.edu.ng).

$$\bar{D}\nabla^4\bar{w}(\tau, \gamma, t) + \mu Ro \frac{\partial^2}{\partial t^2} \bar{w}(\tau, \gamma, t) + Q(\tau)\bar{w}(\tau, \gamma, t) = 2\mu T_r \frac{\partial^4}{\partial \tau^2 \partial \gamma^2} \bar{w}(\tau, \gamma, t) = \bar{P}(\tau, \gamma, t) \quad (1)$$

From (1), \bar{D} represent bending stiffness $\left(\bar{D} = \frac{Eh^3}{12(\bar{\nu})}\right)$ and

$\bar{\nu} = 1 - \nu$, ∇^2 the Laplacian operator in 2-dimensional, t time, Ro rotatory inertia, μ mass of the plate-type, τ & are positions in τ & γ directions, h plate-type thickness, ν the Poisson's ratio, E (Young modulus), $Q(\tau)$ (foundation subgrade) and the Heaviside function is $H(\tau - ct)$.

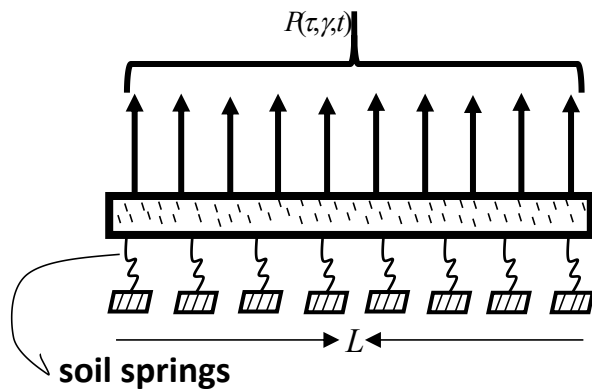


Fig. *1: Loading distributed system on Plate-type

The loading distributed system takes the form

$$\bar{P}(\tau, \gamma, t) = P_m(\tau, \gamma, t) \left\{ 1 - \frac{\Delta^*}{\bar{g}} [\bar{w}(\tau, \gamma, t)] \right\} \quad (2)$$

where \bar{g} , Δ^* and $\bar{P}(\tau, \gamma, t)$ are acceleration due to gravity, acceleration operator, the force moving continuously and moves from a point $\gamma - \gamma_0$. Thus, $P_m(\tau, \gamma, t)$ takes the form

$$P_m(\tau, \gamma, t) = M\bar{g}H(\tau - ct)H(\gamma - \gamma_0) \quad (3)$$

The variable elastic foundation modulus $Q(\tau)$ is given by

$$Q(\tau) = Q_0(4\tau - 3\tau^2 + \tau^3) \quad (4)$$

Time t assumed to be within the interval

$$0 \leq ct \leq L \quad (5)$$

The pertinent boundary conditions for $\tau = 0$ and $\tau = L$ are

$$\bar{w}(\tau, \gamma, t) = 0, \quad \frac{\partial^2 \bar{w}(\tau, \gamma, t)}{\partial \tau^2} = 0 \quad (6)$$

and for $\gamma = 0, \gamma = L$ are

$$\bar{w}(\tau, \gamma, t) = 0, \quad \frac{\partial^2 \bar{w}(\tau, \gamma, t)}{\partial \gamma^2} = 0 \quad (7)$$

The initial conditions are taken to be

$$\bar{w}(\tau, \gamma, t) = 0 = \frac{\partial \bar{w}(\tau, \gamma, t)}{\partial t} \quad (8)$$

Considering equations (2), (3), and (4) in equation (1),

$$\begin{aligned} &\bar{D}\nabla^4\bar{w}(\tau, \gamma, t) + \mu Ro \frac{\partial^2}{\partial t^2} \bar{w}(\tau, \gamma, t) \\ &= 2\mu T_r \frac{\partial^4}{\partial \tau^2 \partial \gamma^2} \bar{w}(\tau, \gamma, t) - Q_0(4\tau - 3\tau^2 + \tau^3)w(\tau, \gamma, t) \\ &\sum_{i=1}^N \left[M_i \bar{g} H(\tau - c_i t) H(\gamma - \gamma_0) - M_i \left(\frac{\partial^2}{\partial t^2} + 2c_i \frac{\partial}{\partial \alpha t} \right. \right. \\ &\left. \left. + c_i^2 \frac{\partial^2}{\partial \gamma^2} \right) \bar{w}(\tau, \gamma, t) H(\tau - c_i t) H(\gamma - \gamma_0) \right] \quad (9) \end{aligned}$$

Equation (9) forms the fundamental model of the plate-type with torsional rigidity on the elastic subgrade.

III. ANALYTICAL PROCEDURES

Clearly, the exact analytical solution for the problem cannot be found. To this end, an approximately analytical procedure (Oni and Ogonyebi [11]) is used. The method is given as

$$\bar{w}(\tau, \gamma, t) = \sum_{k=1}^{\infty} \theta_k(\tau, \gamma) V_k(t) \quad (10)$$

which is the form of [16] and θ_k the eigenfunctions. Also

$$\nabla^4 \theta_k - \omega_k^4 \theta_k = 0 \quad (11)$$

where

$$\omega_k^4 = \frac{\Omega_k^2 \mu}{\bar{D}} \quad (12)$$

and $\Omega_k, k = 1, 2, 3, 4, \dots$, are the natural frequencies & $V_k(t)$ the amplitude to be determined.

Furthermore, let $\theta_k(\tau, \gamma)$ be the products of the functions

β_{kn} and β_{km} (i. e the beam functions in τ and γ)

$$\theta_k(\tau, \gamma) = \beta_{kn}(\tau) \beta_{km}(\gamma) \quad (13)$$

Defining beam functions

$$\begin{aligned} \beta_{kn}(\tau) = & \text{Sin} \frac{\alpha_{kn}\tau}{L_\tau} + A_{kn} \text{Cos} \frac{\alpha_{kn}\tau}{L_\tau} + B_{kn} \text{Sinh} \frac{\alpha_{kn}\tau}{L_\tau} \\ & + C_{kn} \text{Cosh} \frac{\alpha_{kn}\tau}{L_\tau} \quad (14) \end{aligned}$$

and

$$\begin{aligned} \beta_{km}(\gamma) = & \text{Sin} \frac{\alpha_{km}\gamma}{L_\gamma} + A_{km} \text{Cos} \frac{\alpha_{km}\gamma}{L_\gamma} + B_{km} \text{Sinh} \frac{\alpha_{km}\gamma}{L_\gamma} \\ & + C_{km} \text{Cosh} \frac{\alpha_{km}\gamma}{L_\gamma} \quad (15) \end{aligned}$$

where $A_{kn}, B_{kn}, C_{kn}, A_{km}, B_{km}$ & C_{km} are to be determined.

Also, α_{kn} and α_{km} are the mode frequencies.

Re-written equation (9) in the form of a series and applying equation (10), one obtains

$$\sum_{k=1}^{\infty} \left\{ Ro [2T_r (\theta_{k,\tau\tau,\gamma\gamma}(\tau, \gamma) V_k(t) - Q_0(4\tau - 3\tau^2 + \tau^3) \right.$$

$$\begin{aligned} & \cdot \theta_k(\tau, \gamma) V_k(t) + \sum_{i=1}^N \left[\frac{M_i \bar{g}}{\mu} H(\tau - c_i t) H(\gamma - \gamma_0) \right. \\ & - \frac{M_i}{\mu} (\theta_k(\tau, \gamma) V_{k,tt}(t) + 2c_i \theta_{k,x}(\tau, \gamma) V_{k,t}(t) \\ & \left. + c_i^2 \theta_{k,\tau\tau}(\tau, \gamma) V_k(t)) H(\tau - c_i t) H(\gamma - \gamma_0) \right] \\ & = \sum_{k=1}^{\infty} \theta_k(\tau, \gamma) \Phi(t) \end{aligned} \quad (16)$$

where

$$\begin{aligned} \theta_{k,\tau}(\tau, \gamma) & \text{ implies } \frac{\partial \theta_k(\tau, \gamma)}{\partial \tau}, & \theta_{k,\tau\tau}(\tau, \gamma) & \text{ implies } \frac{\partial^2 \theta_k(\tau, \gamma)}{\partial \tau^2} \\ \theta_{k,\gamma}(\tau, \gamma) & \text{ implies } \frac{\partial \theta_k(\tau, \gamma)}{\partial \gamma}, & \theta_{k,\gamma\gamma}(\tau, \gamma) & \text{ implies } \frac{\partial^2 \theta_k(\tau, \gamma)}{\partial \gamma^2} \\ V_{k,t}(t) & \Rightarrow \frac{dV_k(t)}{dt}, & V_{k,tt}(t) & \Rightarrow \frac{d^2 V_k(t)}{dt^2} \end{aligned} \quad (17)$$

Let equation (17) be orthogonal to $\theta_k(\tau, \gamma)$ and integrated to have

$$\begin{aligned} & V_{k,tt}(t) + \frac{D\omega_n^4}{\mu} V(t) \\ & = \frac{1}{\eta} \sum_{r=1}^{\infty} Ro \left\{ \int_A \frac{2T_r}{\mu} [\theta_{r,\tau\tau,\gamma\gamma}(\tau, \gamma) \theta_s(\tau, \gamma) V_r(t) \right. \\ & - \frac{Q_0}{\mu} (4\tau - 3\tau^2 + \tau^3) \theta_r(\tau, \gamma) \theta_s(\tau, \gamma) V_r(t) \\ & + \sum_{i=1}^N \left[\frac{M_i \bar{g}}{\mu} \theta_s(\tau, \gamma) H(\tau - c_i t) H(\gamma - \gamma_0) - \frac{M_i}{\mu} (\theta_r(\tau, \gamma) \right. \\ & \cdot \theta_s(\tau, \gamma) V_{r,tt}(t) + 2c_i \theta_{r,x}(\tau, \gamma) V_{r,t}(t) + c_i^2 \theta_{r,\tau\tau}(\tau, \gamma) \theta_s(\tau, \gamma) V_k(t) \\ & \left. \left. \cdot H(\tau - c_i t) H(\gamma - \gamma_0) \right) \right] \} dA \end{aligned} \quad (18)$$

where

$$\eta = \int_A \theta_s^2 dA$$

By the property of the Heaviside function,

$$H(\tau - c_i t) = \frac{\tau}{L_\tau} + \frac{2}{n\pi} \sum_{i=1}^{\infty} \frac{\sin n\pi x \cos n\pi c_i t}{L_\tau} + C_n \quad (19)$$

$$H(\gamma - \gamma_0) = \frac{\gamma}{L_\gamma} + \frac{2}{m\pi} \sum_{k=1}^{\infty} \frac{\sin m\pi\gamma \cos m\pi\gamma_0}{L_\gamma} + C_n \quad (20)$$

After rearrangements, Equation (18) gives

$$\begin{aligned} & \frac{d^2 V_k(t)}{dt^2} + \Psi_k^2 V_k(t) - \frac{Ro 2T_r H_a^1}{\mu\eta} \sum_{k=1}^{\infty} V_k(t) + \phi_{AA} \sum_{k=1}^{\infty} V_k(t) \\ & - \Upsilon^0 \left[\left(\frac{1}{L_\tau L_\gamma} H_c^{1,1} + \frac{2}{m\pi L_\tau} \sum_{k=1}^{\infty} \frac{\cos m\pi\gamma_0}{L_\gamma} H_c^{1,2}(m) \right) \right. \\ & \left. + \frac{C_n}{L_\tau} H_c^{1,3} + \frac{2}{n\pi L_\gamma} \sum_{n=1}^{\infty} \frac{\cos m\pi c t}{L_\tau} H_c^{1,4}(n) \right. \end{aligned}$$

$$\begin{aligned} & + \frac{4}{nm\pi^2} \sum_{n=1}^{\infty} \sum_{m=1}^{\infty} \frac{\cos n\pi c t}{L_\tau} \frac{\cos m\pi\gamma_0}{L_\gamma} H_c^{1,5}(n, m) \\ & \cdot \frac{2C_n}{n\pi} \sum_{n=1}^{\infty} \frac{\cos n\pi c t}{L_\tau} H_c^{1,6}(n) + \frac{C_n}{L_\gamma} H_c^{1,7} \\ & \left. + \frac{2C_n}{m\pi} \sum_{m=1}^{\infty} \frac{\cos m\pi\gamma_0}{L_\gamma} H_c^{1,8}(m) + C_n^2 H_c^{1,9} \right) \frac{d^2}{dt^2} V_k(t) \\ & + \left(\frac{2c}{L_\tau L_\gamma} H_d^{1,1} + \frac{4}{m\pi L_\tau} \sum_{k=1}^{\infty} \frac{\cos m\pi\gamma_0}{L_\gamma} H_d^{1,2}(m) \right. \\ & + 2c C_n H_d^{1,3} + \frac{4c}{n\pi L_\gamma} \sum_{n=1}^{\infty} \frac{\cos m\pi c t}{L_\gamma} H_d^{1,4}(n) \\ & + \frac{4c}{nm\pi^2} \sum_{n=1}^{\infty} \sum_{m=1}^{\infty} \frac{\cos n\pi c t}{L_\tau} \frac{\cos m\pi\gamma_0}{L_\gamma} H_d^{1,5}(n, m) \\ & + \frac{4c C_n}{n\pi} \sum_{n=1}^{\infty} \frac{\cos n\pi c t}{L_\tau} H_d^{1,6}(n) \\ & \left. + \frac{2c C_n}{L_\gamma} H_d^{1,7} + \frac{4c C_n}{m\pi} \sum_{m=1}^{\infty} \frac{\cos m\pi\gamma_0}{L_\gamma} H_d^{1,8}(m) + 2c C_n^2 H_d^{1,9} \right) \\ & \cdot \frac{d}{dt} V_k(t) + \left(\frac{c^2}{L_\tau L_\gamma} H_e^{1,1} + \frac{2c}{m\pi L_\tau} \sum_{k=1}^{\infty} \frac{\cos m\pi\gamma_0}{L_\gamma} H_e^{1,2}(m) \right. \\ & + \frac{c^2 C_n}{L_\tau} H_e^{1,3} + \frac{2c^2}{n\pi L_\gamma} \sum_{n=1}^{\infty} \frac{\cos m\pi c t}{L_\tau} H_e^{1,4}(n) \\ & + \frac{4c^2}{nm\pi^2} \sum_{n=1}^{\infty} \sum_{m=1}^{\infty} \frac{\cos n\pi c t}{L_\tau} \frac{\cos m\pi\gamma_0}{L_\gamma} H_e^{1,5}(n, m) \\ & + \frac{2c^2 C_n}{n\pi} \sum_{n=1}^{\infty} \frac{\cos n\pi c t}{L_\tau} H_e^{1,6}(n) \\ & + \frac{c^2 C_n}{L_\gamma} H_e^{1,7} + \frac{2c^2 C_n}{m\pi} \sum_{m=1}^{\infty} \frac{\cos m\pi\gamma_0}{L_\gamma} H_e^{1,8}(m) \\ & \left. + c^2 C_n^2 H_e^{1,9} \right) V_k(t) = \frac{M\bar{g}}{\mu\eta} \beta_{kn}(c_i t) \beta_{km}(\gamma_0) \end{aligned} \quad (21)$$

where

$$\Psi_k^2 = \frac{D\omega_n^4}{\mu}, \phi_{AA} = \frac{Q_0 H_b^1}{\mu\eta}, \Upsilon^0 = \frac{1}{L_\tau L_\gamma} \text{ and}$$

$$H_a^1 = \int_0^{L_\tau} \int_0^{L_\gamma} \theta_{r,\tau\tau,\gamma\gamma}(\tau, \gamma) \theta_s(\tau, \gamma) d\gamma d\tau$$

$$H_b^1 = 4R_1 - 3R_1 + R_3$$

$$R_1 = \int_0^{L_x} \int_0^{L_y} x \theta_r(x, y) \theta_s(x, y) dy dx$$

$$R_2 = \int_0^{L_\tau} \int_0^{L_\gamma} \tau^2 \theta_r(\tau, \gamma) \theta_s(\tau, \gamma) d\gamma d\tau$$

$$R_3 = \int_0^{L_\tau} \int_0^{L_\gamma} \tau^3 \theta_r(\tau, \gamma) \theta_s(\tau, \gamma) d\gamma d\tau$$

$$\begin{aligned}
 H_c^{1,1} &= \int_0^{L_x} \int_0^{L_y} \tau \theta_{r,\tau}(\tau, \gamma) \theta_s(\tau, \gamma) d\gamma d\tau \\
 H_c^{1,2} &= \int_0^{L_x} \int_0^{L_y} \tau \frac{\sin m\pi\gamma_0}{L_\gamma} \theta_{r,\tau}(\tau, \gamma) \theta_s(\tau, \gamma) d\gamma d\tau \\
 H_c^{1,3} &= \int_0^{L_x} \int_0^{L_y} \tau \theta_{r,\tau}(\tau, \gamma) \theta_s(\tau, \gamma) d\gamma d\tau \\
 H_c^{1,4} &= \int_0^{L_x} \int_0^{L_y} \gamma \frac{\sin m\pi\tau}{L_\tau} \theta_{r,\tau}(\tau, \gamma) \theta_s(\tau, \gamma) d\gamma d\tau \\
 H_c^{1,5} &= \int_0^{L_x} \int_0^{L_y} \frac{\sin m\pi\tau}{L_\tau} \frac{\sin m\pi\gamma_0}{L_\gamma} \theta_{r,\tau}(\tau, \gamma) \theta_s(\tau, \gamma) d\gamma d\tau \\
 H_c^{1,6} &= \int_0^{L_x} \int_0^{L_y} \frac{\sin m\pi\tau}{L_\tau} \theta_{r,\tau}(\tau, \gamma) \theta_s(\tau, \gamma) d\gamma d\tau \\
 H_c^{1,7} &= \int_0^{L_x} \int_0^{L_y} \gamma \theta_{r,\tau}(\tau, \gamma) \theta_s(\tau, \gamma) d\gamma d\tau \\
 H_c^{1,8} &= \int_0^{L_x} \int_0^{L_y} \frac{\sin m\pi\gamma}{L_\gamma} \theta_{r,\tau}(\tau, \gamma) \theta_s(\tau, \gamma) d\gamma d\tau \\
 H_c^{1,9} &= \int_0^{L_x} \int_0^{L_y} \theta_{r,\tau}(\tau, \gamma) \theta_s(\tau, \gamma) d\gamma d\tau \\
 H_d^{1,1} &= \int_0^{L_x} \int_0^{L_y} \tau \gamma \theta_{r,\tau}(\tau, \gamma) \theta_s(\tau, \gamma) d\gamma d\tau \\
 H_d^{1,2} &= \int_0^{L_x} \int_0^{L_y} \tau \frac{\sin m\pi\gamma}{L_\gamma} \theta_{r,\tau}(\tau, \gamma) \theta_s(\tau, \gamma) d\gamma d\tau \\
 H_d^{1,3} &= \int_0^{L_x} \int_0^{L_y} x \theta_{r,x}(x, y) \theta_s(x, y) dy dx \\
 H_c^{1,4} &= \int_0^{L_x} \int_0^{L_y} \gamma \frac{\sin m\pi\tau}{L_\tau} \theta_{r,\tau}(\tau, \gamma) \theta_s(\tau, \gamma) d\gamma d\tau \\
 H_d^{1,5} &= \int_0^{L_x} \int_0^{L_y} \frac{\sin n\pi\tau}{L_\tau} \frac{\sin m\pi\gamma}{L_\gamma} \theta_{r,\tau}(\tau, \gamma) \theta_s(\tau, \gamma) d\gamma d\tau \\
 H_d^{1,6} &= \int_0^{L_x} \int_0^{L_y} \frac{\sin n\pi\tau}{L_\tau} \theta_{r,\tau}(\tau, \gamma) \theta_s(\tau, \gamma) d\gamma d\tau \\
 H_d^{1,7} &= \int_0^{L_x} \int_0^{L_y} \gamma \theta_{r,\tau}(\tau, \gamma) \theta_s(\tau, \gamma) d\gamma d\tau \\
 H_d^{1,8} &= \int_0^{L_x} \int_0^{L_y} \frac{\sin n\pi\gamma}{L_\gamma} \theta_{r,\tau}(\tau, \gamma) \theta_s(\tau, \gamma) d\gamma d\tau \\
 H_d^{1,9} &= \int_0^{L_x} \int_0^{L_y} \theta_{r,\tau}(\tau, \gamma) \theta_s(\tau, \gamma) d\gamma d\tau \\
 H_e^{1,1} &= \int_0^{L_x} \int_0^{L_y} \tau \gamma \theta_{r,\tau}(\tau, \gamma) \theta_s(\tau, \gamma) d\gamma d\tau \\
 H_e^{1,2} &= \int_0^{L_x} \int_0^{L_y} \tau \frac{\sin n\pi\gamma}{L_\gamma} \theta_{r,\tau}(\tau, \gamma) \theta_s(\tau, \gamma) d\gamma d\tau \\
 H_e^{1,3} &= \int_0^{L_x} \int_0^{L_y} \tau \theta_{r,\tau}(\tau, \gamma) \theta_s(\tau, \gamma) d\gamma d\tau
 \end{aligned}$$

$$\begin{aligned}
 H_e^{1,4} &= \int_0^{L_x} \int_0^{L_y} \gamma \frac{\sin n\pi\tau}{L_\tau} \theta_{r,\tau}(\tau, \gamma) \theta_s(\tau, \gamma) d\gamma d\tau \\
 H_e^{1,5} &= \int_0^{L_x} \int_0^{L_y} \frac{\sin n\pi\tau}{L_\tau} \frac{\sin n\pi\gamma}{L_\gamma} \theta_{r,\tau}(\tau, \gamma) \theta_s(\tau, \gamma) d\gamma d\tau \\
 H_e^{1,6} &= \int_0^{L_x} \int_0^{L_y} \frac{\sin n\pi\tau}{L_\tau} \theta_{r,\tau}(\tau, \gamma) \theta_s(\tau, \gamma) d\gamma d\tau \\
 H_e^{1,7} &= \int_0^{L_x} \int_0^{L_y} \gamma \theta_{r,\tau}(\tau, \gamma) \theta_s(\tau, \gamma) d\gamma d\tau \\
 H_e^{1,8} &= \int_0^{L_x} \int_0^{L_y} \frac{\sin n\pi\gamma}{L_\gamma} \theta_{r,\tau}(\tau, \gamma) \theta_s(\tau, \gamma) d\gamma d\tau \\
 H_e^{1,9} &= \int_0^{L_x} \int_0^{L_y} \theta_{r,\tau}(\tau, \gamma) \theta_s(\tau, \gamma) d\gamma d\tau
 \end{aligned}$$

A. Plate-type moving distributed force procedure

Setting $\Upsilon^0 = 0$ in equation (21), the deflecting model (Plate-type) lying on the subgrade is addressed. Therefore, if $\Upsilon^0 = 0$, one obtains

$$\begin{aligned}
 &\frac{d^2 V_k(t)}{dt^2} + \Psi_k^2 V_k(t) - \frac{Ro2T_r H_a^1}{\mu\eta} \sum_{k=1}^{\infty} V_r(t) + \varphi_{AA} \sum_{k=1}^{\infty} V_k(t) \\
 &= \frac{Mg}{\mu\eta} \beta_{kn}(ct) \beta_{km}(y_0) \tag{22}
 \end{aligned}$$

Struble's technique is then employed to solve equation (22) and the foundation subgrade term is neglected first so that equation (22) is further arranged to take the shape

$$\begin{aligned}
 &\frac{d^2 V_k(t)}{dt^2} + (\Psi_k^2 + \Upsilon^o H_a^1) V_k(t) \\
 &+ \Upsilon^o H_a^1 \sum_{r=1}^{\infty} V_r(t) = \frac{Mg}{\mu\eta} \beta_{kn}(ct) \beta_{km}(y_0) \tag{23}
 \end{aligned}$$

where

$$\Upsilon^o = \frac{2T_r}{\mu\eta} \tag{24}$$

Thus, consideration of ξ where ($\xi < 1$) for the arbitrary ratio Υ^o i.e

$$\xi = \frac{\Upsilon^o}{1 + \Upsilon^o} \tag{25}$$

$$\Upsilon^o = \xi + 0(\xi^2) \tag{26}$$

Putting equation (26) in equation (23) gives

$$\frac{d^2 V_k(t)}{dt^2} + (\Psi_k^2 + \xi H_a^1) V_k(t) + \xi H_a^1 \sum_{r=1}^{\infty} V_r(t) = 0 \tag{27}$$

Also set $\xi = 0$ in (27), the effect of the torsional rigidity is ignored and the solution is written as

$$V_k(t) = C_o \cos[\Psi_k(t) - \phi] \tag{28}$$

Where C_o , ϕ and Ψ_k are constants and it is noted that

$$V_k(t) = \varphi_k(t) \cos[\Psi_k t - \phi(t)] + \xi V_1(t) + 0(\xi^2) \tag{29}$$

where $\varphi_k(t)$ & $\phi(t)$ are slowly varying functions.

$$\frac{d\varphi_k(t)}{dt} \text{ is of } 0(\xi), \quad \frac{d^2\varphi_k(t)}{dt^2} \text{ is of } 0(\xi^2) \quad (30)$$

$$\frac{d\phi(t)}{dt} \text{ is of } 0(\xi), \quad \frac{d^2\phi(t)}{dt^2} \text{ is of } 0(\xi^2) \quad (31)$$

Therefore, replacing equation (27) with

$$\frac{d^2V_k(t)}{dt^2} + \Omega_f^2 V_k(t) = 0 \quad (32)$$

where

$$\Omega_f = \Psi_k + \frac{\xi H_a^1}{2\Psi_k} \quad (33)$$

which is modified frequency with respect to the influence of torsional rigidity. Furthermore, setting $\xi = 0$, it is evident that the frequency of the MF problem is recovered when the influence of torsional rigidity is neglected. Thus

$$\frac{d^2V_k(t)}{dt^2} + \Omega_f^2 V_k(t) + \frac{Q_0 H_b^1}{\mu\eta} \sum_{k=1}^{\infty} V_k(t) = \frac{Mg}{\mu\eta} \beta_{kn}(ct) \beta_{kn}(\gamma) \quad (34)$$

Again, rearranging

$$\frac{d^2V_k(t)}{dt^2} + \Omega_f^2 V_k(t) + \gamma_o H_b^1 \frac{dV_k(t)}{dt} - \mathcal{G}_o H_b^1 \sum_{\substack{k=1 \\ k \neq n}}^{\infty} \frac{dV_k(t)}{dt} = 0 \quad (35)$$

where

$$\mathcal{G}_o = \frac{Q_0}{\eta} \quad (36)$$

consider the parameter β_{ii} (for subjective ratio \mathcal{G}_o) therefore,

$$\beta_{ii} = \frac{\mathcal{G}_o}{1 + \mathcal{G}_o} \quad (37)$$

Hence,

$$\mathcal{G}_o = \beta_{ii} + 0(\beta_{ii}^2) \quad (38)$$

So that equation (35) is replaced by

$$\frac{d^2V_k(t)}{dt^2} + \Omega_{fm}^2 V_k(t) = 0 \quad (39)$$

where

$$\Omega_{fm} = \Omega_f \left(\frac{1 + H_a^1}{2} \right) \quad (40)$$

To obtain a solution to equation (34) $V_k(t)$ is replaced with the new modified frequency (NMF) of equation (40). Thus,

$$\frac{d^2V_k(t)}{dt^2} + \Omega_{fm}^2 V_k(t) = \frac{Mg}{\mu\eta} \beta_{kn}(ct) \beta_{kn}(\gamma_0) \quad (41)$$

which is further rearranged as

$$\frac{d^2V_k(t)}{dt^2} + \Omega_{fm}^2(t) = G_{mf} L_\tau L_\gamma \cdot \left[-\text{Cos} \chi_k + A_{kn} \text{Sin} \chi_k + B_{kn} \text{Cosh} \chi_k + C_{kn} \text{Sinh} \chi_k + \text{Cos} \frac{\chi_n ct}{L_\tau} + A_{kn} \text{Sin} \frac{\chi_n ct}{L_\tau} + B_{kn} \text{Cosh} \frac{\chi_n ct}{L_\tau} + C_{kn} \text{Sinh} \frac{\chi_n ct}{L_\tau} \right]$$

$$+ B_{km} \text{Cosh} \chi_k + C_{km} \text{Sinh} \chi_k + \text{Cos} \frac{\chi_k \gamma}{L_\gamma} + A_{km} \text{Sin} \frac{\chi_k \gamma}{L_\gamma} + B_{km} \text{Cosh} \frac{\chi_k \gamma}{L_\gamma} + C_{km} \text{Sinh} \frac{\chi_k \gamma}{L_\gamma} \quad (42)$$

where

$$G_{mf} = \frac{Mg}{\mu\eta knkm}, \quad \chi_k = \alpha_{km}, \quad \chi_n = \alpha_{kn} \quad (43)$$

When equation (42) is solved taking into account equation (8), one obtains an expression for $V_k(t)$ and considering equation (10) in equation (42), one obtains

$$\bar{w}(\tau, \gamma, t) = G_{mf} L_\tau L_\gamma \sum_{kn=1}^{\infty} \sum_{km=1}^{\infty} \varepsilon_o(\gamma) \times \left\{ G_{mg} \varepsilon_1 \sin \Omega_{fm} t \frac{\sin a_{kn} t + \sin \Omega_{fm} t}{\Omega_{fm}^2 - a_{kn}^2} - \frac{\cos a_{kn} t + \cos \Omega_{fm} t}{\Omega_{fm}^2 - a_{kn}^2} \frac{B_{kn} 2\Omega_{fm}^2 a_{kn} \sin 2\Omega_{fm} t \cosh a_{kn} t}{\Omega_{fm}^4 - a_{kn}^4} - \frac{B_{kn} a_{kn}^2 \cos 2\Omega_{fm} t \sin a_{kn} t}{\Omega_{fm}^4 - a_{kn}^4} + \frac{B_{kn} a_{kn} \sin \Omega_{fm} t (a_{kn}^2 - \Omega_{fm}^2)}{\Omega_{fm}^4 - a_{kn}^4} - \frac{C_{kn} 2\Omega_{fm}^2 a_{kn} \sin 2\Omega_{fm} t \sinh a_{kn} t}{\Omega_{fm}^4 - a_{kn}^4} + \frac{C_{kn} a_{kn}^2 \cos 2\Omega_{fm} t \mathcal{G}_b}{\Omega_{fm}^4 - a_{kn}^4} + \frac{C_{kn} \Omega_{fm}^2 \cosh a_{kn} t}{\Omega_{fm}^4 - a_{kn}^4} + \frac{C_{kn} (a_{kn}^2 - \Omega_{fm}^2)}{\Omega_{fm}^4 - a_{kn}^4} \right\} \times \beta_{kn}(\tau) \beta_{kn}(\gamma) \quad (44)$$

where

$$G_{mg} = -\frac{1}{\Omega_{fm}} \quad (45)$$

$$\varepsilon_o(\gamma) = -\cos \alpha_{km} + A_{km} \sin \alpha_{km} + B_{km} \cosh \alpha_{km} + C_{km} \sinh \alpha_{km} + \cos \frac{\alpha_{km} \gamma}{L_\gamma} + A_{km} \sin \frac{\alpha_{km} \gamma}{L_\gamma} + B_{km} \cosh \frac{\alpha_{km} \gamma}{L_\gamma} + C_{km} \sinh \frac{\alpha_{km} \gamma}{L_\gamma} \quad (46)$$

$$\varepsilon_1 = -\cos \alpha_{kn} + A_{kn} \sin \alpha_{kn} + B_{kn} \cosh \alpha_{kn} + C_{kn} \sinh \alpha_{kn} \quad (47)$$

$$a_{kn} = \frac{\alpha_{kn} c}{L_\tau} \quad (48)$$

The new equation of the plate-type model for MDF lying on constant subgrade is aptly given in equation (44).

B. Plate-type moving distributed force procedure

When $\Upsilon \neq 0$, the solution to the entire equation (21) is presented. Therefore, arrangements of equation (21) give

$$\frac{d^2V_k(t)}{dt^2} + \Omega_{fm}^2 V_k(t) + \frac{\Upsilon^*}{\eta} \sum_{r=1}^{\infty} \tau \gamma H_c^{1,1} + \frac{2}{m\pi L_\tau} \sum_{k=1}^{\infty} \frac{\cos m\pi\gamma}{L_\gamma} \cdot H_c^{1,2}(m) + C_n L_\tau \tau H_c^{1,3} + \frac{2L_\tau}{n\pi L_\gamma} \sum_{n=1}^{\infty} \frac{\cos n\pi ct}{L_\tau} H_c^{1,4}(n)$$

$$\begin{aligned}
 & + \frac{4L_\tau L_\gamma}{nm\pi^2} \sum_{n=1}^{\infty} \sum_{m=1}^{\infty} \frac{\cos n\pi ct}{L_\tau} \frac{\cos m\pi\gamma}{L_\gamma} H_c^{1,5}(n, m) \\
 & + \frac{2C_n L_\tau L_\gamma}{n\pi} \sum_{n=1}^{\infty} \frac{\cos n\pi ct}{L_\tau} H_c^{1,6}(n) + C_n \gamma L_\tau H_c^{1,7} \\
 & + \frac{2C_n}{m\pi} \sum_{m=1}^{\infty} \frac{\cos m\pi\gamma}{L_\gamma} H_c^{1,8}(m) + C_n^2 L_\tau L_\gamma H_c^{1,9} \left) \frac{d^2}{dt^2} V_k(t) \right. \\
 & + 2c \left(x\gamma H_d^{1,1} + \frac{2\tau}{m\pi L_\tau} \sum_{k=1}^{\infty} \frac{\cos m\pi\gamma}{L_\gamma} H_d^{1,2}(m) \right. \\
 & \cdot + 2cC_n H_d^{1,3} + \frac{2\gamma}{n\pi} \sum_{n=1}^{\infty} \frac{\cos m\pi ct}{L_\tau} H_d^{1,4}(m) + \frac{4L_\tau L_\gamma}{nm\pi^2} \\
 & \cdot \sum_{n=1}^{\infty} \sum_{m=1}^{\infty} \frac{\cos n\pi ct}{L_\tau} \frac{\cos m\pi\gamma}{L_\gamma} H_d^{1,5}(n, m) + \frac{4cC_n}{n\pi} \sum_{n=1}^{\infty} \frac{\cos n\pi ct}{L_\tau} \\
 & \cdot H_d^{1,6}(n) + C_n L_\tau \gamma H_d^{1,7} + \varphi_{A1} \sum_{m=1}^{\infty} \frac{\cos m\pi\gamma}{L_\gamma} H_d^{1,8}(n, m) + C_n^2 L_\tau L_\gamma H_d^{1,9} \left. \right) \\
 & \cdot \frac{d}{dt} V_k(t) + c^2 \left(\tau\gamma H_e^{1,1} + \frac{2xL_\tau}{m\pi} \sum_{m=1}^{\infty} \frac{\cos m\pi\gamma}{L_\gamma} H_e^{1,2}(m) \right. \\
 & + C_n L_\tau \tau H_e^{1,3} + \frac{2\gamma L_\gamma}{n\pi} \sum_{n=1}^{\infty} \frac{\cos m\pi ct}{L_\tau} H_e^{1,4}(m) + \frac{4L_\gamma}{nm\pi^2} \\
 & \cdot \sum_{n=1}^{\infty} \sum_{m=1}^{\infty} \frac{\cos n\pi ct}{L_\tau} \frac{\cos m\pi\gamma}{L_\gamma} H_e^{1,5}(n, m) + \varphi_{A2} \sum_{n=1}^{\infty} \frac{\cos n\pi ct}{L_\tau} H_e^{1,6}(n) \\
 & + \frac{c^2 C_n}{L_\gamma} H_e^{1,7} + \varphi_{A3} \sum_{m=1}^{\infty} \frac{\cos m\pi\gamma}{L_\gamma} H_e^{1,8} + c^2 C_n^2 H_e^{1,9} \left. \right) V_r(t) \left. \right] \\
 & = \frac{Mg}{\mu\eta} \beta_{kn}(ct) \beta_{km}(\gamma) \tag{49}
 \end{aligned}$$

where

$$\Upsilon^* = \frac{1}{L_\tau L_\gamma}, \varphi_{A1} = \frac{2C_n}{m\pi}, \varphi_{A2} = \frac{2L_\tau C_n}{n\pi}, \varphi_{A3} = \frac{2c^2 C_n}{m\pi}$$

Further arrangements of (49) is

$$\begin{aligned}
 & \frac{d^2 V_k(t)}{dt^2} + \frac{\Upsilon^* G_{m1}(t)}{1 + \Upsilon^* G_{mo}(t)} \frac{dV_k(t)}{dt} + \frac{\Omega_{fm}^2 + \Upsilon^* G_{m2}(t)}{1 + \Upsilon^* G_{mo}(t)} V_k(t) \\
 & + \frac{\Upsilon^*}{1 + \Upsilon^* G_{mo}(t)} \sum_{r=1}^{\infty} \left[G_{mo}(t) + \frac{d^2 V_r(t)}{dt^2} + G_{m1}(t) \frac{dV_r(t)}{dt} \right. \\
 & \left. + G_{m2}(t) V_r(t) \right] = \frac{\Upsilon^* Mg}{\mu\eta (1 + \Upsilon^* G_{mo}(t))} \beta_{kn}(ct) \beta_{km}(y_0) \tag{50}
 \end{aligned}$$

where

$$\begin{aligned}
 G_{mo}(t) & = \frac{1}{\eta} \left[H_c^{1,1} + \varphi_{A4} \sum_{k=1}^{\infty} \vartheta_a H_c^{1,2}(m) + C_n L_\tau \tau H_c^{1,3} \right. \\
 & + \varphi_{A5} \sum_{n=1}^{\infty} \frac{\cos n\pi ct}{L_\tau} H_c^{1,4}(n) + \varphi_{A6} \sum_{n=1}^{\infty} \sum_{m=1}^{\infty} \frac{\cos n\pi ct}{L_\tau} \vartheta_a \\
 & \times H_c^{1,5}(n, m) + \varphi_{A7} \sum_{n=1}^{\infty} \frac{\cos n\pi ct}{L_\tau} H_c^{1,6}(n) + C_n \gamma L_\tau H_c^{1,7} \\
 & \left. + \frac{2C_n}{m\pi} \sum_{m=1}^{\infty} \frac{\cos m\pi\gamma}{L_\gamma} H_c^{1,8}(m) + C_n^2 L_\tau L_\gamma H_c^{1,9} \right] \\
 G_{m1}(t) & = \frac{2c}{\eta} \left[\tau\gamma H_d^{1,1} + \varphi_{A4} \sum_{k=1}^{\infty} \vartheta_a H_d^{1,2}(m) + 2cC_n H_d^{1,3} \right. \\
 & + \frac{2\gamma L_\gamma}{n\pi L_\tau} \sum_{n=1}^{\infty} \frac{\cos m\pi ct}{L_\tau} H_d^{1,4}(m) + \frac{4L_\tau L_\gamma}{nm\pi^2} \\
 & \times \sum_{n=1}^{\infty} \sum_{m=1}^{\infty} \frac{\cos n\pi ct}{L_\tau} \vartheta_a H_d^{1,5}(n, m) + \frac{4cC_n}{n\pi} \sum_{n=1}^{\infty} \frac{\cos n\pi ct}{L_\tau} H_d^{1,6}(n) \\
 & \left. + C_n L_\tau \gamma H_d^{1,7} + \frac{2C_n}{m\pi} \sum_{m=1}^{\infty} \vartheta_a H_d^{1,8}(n, m) + C_n^2 L_\tau L_\gamma H_d^{1,9} \right] \\
 G_{m2}(t) & = \frac{c^2}{\eta} \left[\tau\gamma H_e^{1,1} + \frac{2xL_\tau}{n\pi} \sum_{n=1}^{\infty} \vartheta_a H_e^{1,2}(m) + C_n L_\tau \tau H_e^{1,3} + \frac{2\gamma L_\gamma}{n\pi} \sum_{n=1}^{\infty} \vartheta_a H_e^{1,4}(m) \right. \\
 & + \varphi_{A9} \sum_{n=1}^{\infty} \sum_{m=1}^{\infty} \frac{\cos n\pi ct}{L_\tau} \vartheta_a H_e^{1,5}(n, m) + \varphi_{A8} \sum_{n=1}^{\infty} \frac{\cos n\pi ct}{L_\tau} H_e^{1,6}(n) \\
 & \left. + \frac{c^2 C_n}{L_\gamma} H_e^{1,7} + \frac{2c^2 C_n}{m\pi} \sum_{m=1}^{\infty} \vartheta_a H_e^{1,8}(m) + c^2 C_n^2 H_e^{1,9} \right]
 \end{aligned}$$

and

$$\begin{aligned}
 \varphi_{A4} & = \frac{2}{m\pi L_\tau}, \varphi_{A5} = \frac{2L_\tau}{n\pi L_\gamma}, \varphi_{A6} = \frac{4L_\tau L_\gamma}{nm\pi^2}, \varphi_{A7} = \frac{2C_n L_\tau L_\gamma}{n\pi} \\
 \vartheta_a & = \frac{\cos m\pi\gamma}{L_\gamma}, \varphi_{A8} = \frac{2L_\tau C_n}{n\pi}, \varphi_{A9} = \frac{4L_\gamma}{nm\pi^2}
 \end{aligned}$$

Following the same procedures as recently discussed, the new modified frequency (NMF) for moving mass problem is

$$\varphi_{mm} = \Omega_{fm} \left(1 - \beta^0 / 2 \left(G_{mo} - G_{m2} / \Omega_{fm}^2 \right) \right) \tag{51}$$

retaining terms to $O(\beta^0)$ only.

The solution to non-homogeneous equation (50) is replaced with the new modified frequency in equation (51) to have

$$\begin{aligned}
 & \frac{d^2 V_k(t)}{dt^2} + \varphi_{mm}^2(t) = G_{nm} L_\tau L_\gamma \left[-\cos \chi_n + A_{kn} \sin \chi_n \right. \\
 & \left. + B_{kn} \cosh \chi_n + C_{kn} \sinh \chi_n + \cos \frac{\chi_n ct}{L_\tau} + A_{kn} \sin \frac{\chi_n ct}{L_\tau} \right]
 \end{aligned}$$

$$\begin{aligned}
 &+B_{kn} \cosh \frac{\chi_n ct}{L_\tau} + C_{kn} \sinh \frac{\chi_n ct}{L_\tau} \left] \times \left[-\cos \chi_k + A_{km} \sin \chi_k \right. \\
 &+B_{km} \cosh \chi_k + C_{km} \sinh \chi_k + B_{km} \cosh \frac{\chi_k \gamma}{L_\gamma} \\
 &\left. + \cos \frac{\chi_k \gamma}{L_\gamma} + A_{km} \sin \frac{\chi_k \gamma}{L_\gamma} + C_{km} \sinh \frac{\chi_k \gamma}{L_\gamma} \right] \quad (52)
 \end{aligned}$$

where

$$G_{mm} = \frac{Mg\beta^0}{\mu\eta\kappa nkm} \quad (53)$$

Obviously, equation (52) is similar to equation (42) and when solved considering initial conditions gives

$$\begin{aligned}
 \bar{w}(\tau, \gamma, t) = &G_{mf} L_\tau L_\gamma \sum_{kn=1}^{\infty} \sum_{km=1}^{\infty} \varepsilon_o(\gamma) \left\{ G_{mg} \varepsilon_1 \sin \varphi_{mm} t \right. \\
 &\frac{\sin a_{kn} t + \sin \varphi_{mm} t}{\varphi_{mm}^2 - a_{kn}^2} - \frac{\cos a_{kn} t + \cos \varphi_{mm} t}{\varphi_{mm}^2 - a_{kn}^2} \\
 &\frac{B_{kn} 2\varphi_{mm}^2 a_{kn} \sin 2\varphi_{mm} t \vartheta_b}{\varphi_{mm}^4 - a_{kn}^4} - \frac{B_{kn} a_{kn}^2 \cos 2\varphi_{mm} t \vartheta_c}{\varphi_{mm}^4 - a_{kn}^4} \\
 &+ \frac{B_{kn} \varphi_{mm}^2 \sin a_{kn} t}{\varphi_{mm}^4 - a_{kn}^4} + \frac{B_{kn} a_{kn} \sin \varphi_{mm} t (a_{kn}^2 - \varphi_{mm}^2)}{\varphi_{mm}^4 - a_{kn}^4} \\
 &\left. - \frac{C_{kn} 2\varphi_{mm}^2 a_{kn} \sin 2\varphi_{mm} t \vartheta_c}{\varphi_{mm}^4 - a_{kn}^4} + \frac{C_{kn} a_{kn}^2 \cos 2\varphi_{mm} t \vartheta_b}{\varphi_{mm}^4 - a_{kn}^4} \right. \\
 &\left. + \frac{C_{kn} \varphi_{mm}^2 \vartheta_b}{\varphi_{mm}^4 - a_{kn}^4} + \frac{C_{kn} (a_{kn}^2 - \varphi_{mm}^2)}{\varphi_{mm}^4 - a_{kn}^4} \right\} \times \beta_{kn}(\tau) \beta_{km}(\gamma) \quad (54)
 \end{aligned}$$

where $\vartheta_b = \cosh a_{kn} t$, $\vartheta_c = \sin a_{kn} t$

Equation (54) is the transverse vibrational response to MDM of the plate-type resting on variable foundation subgrade at a constant speed.

IV. APPLICATIONS

A. Plate-type Clamped at edges $\tau = 0, \tau = L_\tau$ with

simple edges $\gamma = 0, \gamma = L_\gamma$

Here,

$$\begin{aligned}
 \bar{w}(0, \gamma, t) = 0, \quad \bar{w}(L_\tau, \gamma, t) = 0 \\
 \bar{w}(\tau, 0, t) = 0, \quad \bar{w}(\tau, L_\gamma, t) = 0 \quad (55)
 \end{aligned}$$

$$\begin{aligned}
 \frac{\partial \bar{w}(0, \gamma, t)}{\partial \tau} = 0, \quad \frac{\partial \bar{w}(L_\tau, \gamma, t)}{\partial \tau} = 0 \\
 \frac{\partial \bar{w}(0, \tau, t)}{\partial \gamma} = 0, \quad \frac{\partial \bar{w}(\tau, L_\gamma, t)}{\partial \gamma} = 0 \quad (56)
 \end{aligned}$$

and therefore,

$$\begin{aligned}
 \beta_{sn}(0) = 0, \quad \beta_{sn}(L_\tau) = 0, \\
 \beta_{sm}(0) = 0, \quad \beta_{sm}(L_\gamma) = 0 \quad (57) \\
 \frac{\partial \beta_{sn}(0)}{\partial \tau} = 0, \quad \frac{\partial \beta_{sn}(L_\tau)}{\partial \tau} = 0
 \end{aligned}$$

$$\frac{\partial \beta_{sm}(0)}{\partial \gamma^2} = 0, \quad \frac{\partial \beta_{sm}(L_\tau)}{\partial \gamma^2} = 0 \quad (58)$$

The IC's are given by equation (8). Using the BC's (55) and (56), one obtains for clamped edge $x = 0$ and $x = L_\tau$

$$A_{kn} = -\frac{B_1 - \sin z_{kn}}{B_2 - \cos z_{kn}} \Rightarrow A_{sn} = -\frac{B_3 - \sin z_{sn}}{B_4 - \cos z_{sn}} \quad (59)$$

where $B_1 = \sinh z_{kn}, B_2 = \cosh z_{kn}$

$B_3 = \sinh z_{sn}, B_4 = \cosh z_{sn}$

$$B_{rm} = -1 \Rightarrow B_{sm} = -1 \quad (60a)$$

$$C_{rm} = -A_{rm} \Rightarrow C_{sm} = -A_{sm} \quad (60b)$$

The determinant below gives the FE (frequency of the model) for the CC-edges

$$\begin{vmatrix} \cos z_{kn} - \cosh z_{kn} & \sin z_{kn} - \sinh z_{kn} \\ \sin z_{kn} + \sinh z_{kn} & -\cos z_{kn} - \cosh z_{kn} \end{vmatrix} = 0 \quad (60c)$$

which when simplified gives

$$\cosh z_{kn} \cos z_{kn} - 1 = 0 \quad (61)$$

such that

$$z_{1n} = 4.73004, z_{2n} = 7.85320, z_{3n} = 10.99561 \quad (62)$$

and

$$\begin{aligned}
 \bar{w}_{sn} = &\frac{\mu L_\tau}{2} \left\{ 1 + A_{sn}^2 - B_{sn}^2 + C_{sn}^2 + \frac{1}{z_{sn}} [2C_{sn} - 2A_{sn} B_{sn} \right. \\
 &- B_{pi} C_{pi} - \frac{1}{2}(1 - A_{sn}^2) \sin 2z_{sn} + 2A_{sn} \sin^2 z_{sn} \\
 &+ (B_{sn}^2 + C_{sn}^2) \sinh z_{sn} \cosh z_{sn} + 2(B_{sn} + A_{sn} C_{sn}) \\
 &\times \cosh z_{sn} \sin z_{sn} + 2(-B_{sn} + A_{sn} C_{sn}) \sinh z_{sn} \cos z_{sn} \\
 &+ 2(C_{sn} + A_{sn} B_{sn}) \sinh z_{sn} \sin z_{sn} + 2(-C_{sn} + A_{sn} B_{sn}) \\
 &\left. \times \cosh z_{sn} \cos z_{sn} + B_{sn} C_{sn} \cosh z_{sn} \right\} \quad (63)
 \end{aligned}$$

Replacing n by m in (63), clearly, one obtains \bar{w}_{sm} . And,

$$A_{km} = 0 \Rightarrow A_{sm} = 0 \quad (64)$$

$$B_{km} = 0 \Rightarrow B_{sm} = 0 \quad (65)$$

$$C_{km} = 0 \Rightarrow C_{sm} = 0 \quad (66)$$

while the corresponding FE is

$$z_{kn} = km\pi \Rightarrow z_{sm} = sm\pi$$

$$\text{and } \bar{w}_{sm} = \frac{\mu L_\gamma}{2} \quad (67)$$

Therefore, the fundamental solutions for MDM & MDF for the plate-type are achieved by putting obtained results in equations (59) - (67) into equations (44) & (54) respectively.

B. All edges Clamped Plate-type

Here, the slope & deflection easily vanish here. So,

$$\bar{w}(0, \gamma, t) = 0, \quad \bar{w}(L_\tau, \gamma, t) = 0$$

$$\bar{w}(\tau, 0, t) = 0, \bar{w}(\tau, L_\gamma, t) = 0 \tag{68}$$

$$\frac{\partial \bar{w}(0, \gamma, t)}{\partial \tau} = 0, \frac{\partial \bar{w}(L_\tau, \gamma, t)}{\partial \tau} = 0$$

$$\frac{\partial \bar{w}(\tau, 0, t)}{\partial \gamma} = 0, \frac{\partial \bar{w}(\tau, L_\tau, t)}{\partial \gamma} = 0 \tag{69}$$

and therefore,

$$\beta_{sn}(0) = 0, \beta_{sn}(L_\tau) = 0,$$

$$\beta_{sm}(0) = 0, \beta_{sm}(L_\gamma) = 0 \tag{70}$$

$$\frac{\partial \beta_{sn}(\bar{w})}{\partial \tau} = 0, \frac{\partial \beta_{sn}(L_\tau)}{\partial \tau} = 0$$

$$\frac{\partial \beta_{sm}(0)}{\partial \gamma} = 0, \frac{\partial \beta_{sm}(L_\tau)}{\partial \gamma} = 0 \tag{71}$$

with the same initial conditions in (68) to (71) in the plate-type functions, one obtains for clamped edges

$$A_{kn} = -\frac{B_1 - \sin z_{kn}}{B_2 - \cos z_{kn}} \Rightarrow A_{sn} = -\frac{B_3 - \sin z_{sn}}{B_4 - \cos z_{sn}} \tag{72}$$

$$B_{rm} = -1 \Rightarrow B_{sm} = -1 \tag{73}$$

$$C_{rm} = -A_{rm} \Rightarrow C_{sm} = -A_{sm} \tag{74}$$

The determinant in (75) gives the FE (frequency equation) of CC- edges of the plate-type

$$\begin{vmatrix} \cos z_{kn} - \cosh z_{kn} & \sin z_{kn} - \sinh z_{kn} \\ \sin z_{kn} + \sinh z_{kn} & -\cos z_{kn} - \cosh z_{kn} \end{vmatrix} = 0 \tag{75}$$

which when simplified gives

$$\cosh z_{kn} \cos z_{kn} - 1 = 0 \tag{76}$$

such that

$$z_{1n} = 4.73004, z_{2n} = 7.85320, z_{3n} = 10.99561 \tag{77}$$

It follows that for the p_j^{th} mode of vibration

$$\cosh z_{sm} \cos z_{sm} - 1 = 0 \tag{78}$$

Similarly, for the clamped edges, $\gamma = 0$ and $\gamma = L_\gamma$

$$A_{kn} = -\frac{B_1 - \sin z_{kn}}{B_2 - \cos z_{kn}} \Rightarrow A_{sn} = -\frac{B_3 - \sin z_{sn}}{B_4 - \cos z_{sn}} \tag{79}$$

$$B_{rm} = -1 \Rightarrow B_{sm} = -1 \tag{80a}$$

and

$$C_{rm} = -A_{rm} \Rightarrow C_{sm} = -A_{sm} \tag{80b}$$

The determinant in (81) gives the FE (frequency equation) of CC-edges of the plate-type

$$\begin{vmatrix} \cos z_{sm} - \cosh z_{sm} & \sin z_{sm} - \sinh z_{sm} \\ \sin z_{sm} + \sinh z_{sm} & -\cos z_{sm} - \cosh z_{sm} \end{vmatrix} = 0 \tag{81}$$

which when simplified yields

$$\cosh z_{sm} \cos z_{sm} - 1 = 0 \tag{82}$$

Similarly, for p_i^{th} mode of vibration, we have

$$\cosh z_{sn} \cos z_{sn} - 1 = 0 \tag{83}$$

Using arguments similar to the previous one \bar{w}_{sn} is given

by the equation (63) when the values of constants A_{sm} , B_{sm} , C_{sm} and z_{sm} are approximately substituted into the equation. β_{sm} is obtained by replacing subscript sn with sm in equation (63).

V. PLATE-TYPE ANALYSIS AND RESONANCE EFFECT

This section examines the occurrences of the resonating effects of the plate-type. For MDF,

$$\Omega_{fm} = \frac{\alpha_{kn}c}{L_\tau} \tag{84}$$

Also, equation (54) exhibit similar action for MDM system and

$$\varphi_{mm} = \frac{\alpha_{kn}c}{L_\tau} \tag{85}$$

where

$$\varphi_{mm} = \Omega_{fm} \left(1 - \beta^0 / 2 \left(G_{m0} - G_{m2} / \Omega_{fm}^2 \right) \right) \tag{86}$$

Equations (85) and (86) imply

$$\varphi_{mm} = \Omega_{fm} \left(1 - \beta^0 / 2 \left(G_{m0} - G_{m2} / \Omega_{fm}^2 \right) \right) = \frac{\alpha_{kn}c}{L_x} \tag{87}$$

A deduction from (84) & (87) predicts that MDM is smaller than the MDF having considered smaller NF (natural frequency) and CS (critical speed).

VI. PLATE-TYPE RESULTS AND DISCUSSION

As an illustration, an example of a plate-type having length L_τ , L_γ & c defined as, 0.91m, 0.457m & 8.123m/s (lengths L_τ , L_γ & velocity) is considered. Furthermore, parameters γ , α , E , & Y are 0.4m, $3.109 \times 10^9 \text{ kg/m}^2$, .02 & 2.

Following the analytical procedures adopted in this paper, a computer program was created to study the behavioral magnitude of the plate-type with distributed loads on an elastic subgrade. Results are aptly presented in curves as given below. Figure 1 displays the transverse displacement response to plate-type simple-clamped end conditions under the action of MDF for an elastic foundation Q_0 . Observations when T_r & R_0 (torsional rigidity & rotatory inertia) are fixed give a rise in the values of elastic subgrade thereby giving rise to a reduction in the vibration magnitude for simple-clamped plate-type. Curves in (2) depict the magnitude of plate-type SC-ends end condition moved by MDM for elastic subgrade Q_0 . Similarly, a rise in subgrade values produces a decrease in the plate-type profiles at fixed values of torsional rigidity T_r and rotatory inertia R_0 .

Figure 3 shows the influence of torsional rigidity T_r on the vibration of plate-type simple-clamped end condition traversed by MDF at a constant speed. Evidently, when Q_0 & R_0 are fixed, an increase in the torsional rigidity

results in a decrease in the displacement of the plate-type structure.

Figure 4 depicts the effect of torsional rigidity T_r on the flexural motions of plate-type simple-clamped traversed by MDF at a constant speed. Clearly, higher values of torsional rigidity T_r produce a decrease in the deflection profile of the structural member.

Figure 5 and figure 6 display the dynamic deflections of simple-clamped plate end conditions under the action of MDF and MDM systems for varying R_0 and when T_r & are fixed. In a similar manner, a rise in R_0 produces a reduction in the profile of the plate-type structure.

A good comparison is made for MDF and MDM of the plate-type SC-end at edges $\tau = 0, \tau = L_r$ with simple edges $\gamma = 0, \gamma = L_r$ for constant values of Q_0, R_0 and T_r is given in figure 7.

Displacement response to plate-type clamped-clamped end conditions traversed by MDF for an elastic foundation Q_0 is given in figure 8. Observations from the profiles show that when T_r & R_0 are fixed, a rise in the magnitude of Q_0 gives a reduction in magnitude of the 2-dimensional members.

Figure 9 illustrates the deflection of plate-type clamped-clamped end condition traversed by MDM for elastic foundation Q_0 . Similarly, a rise in magnitude of elastic subgrade produces a decrease in the profile of 2-dimensional members at fixed values of torsional rigidity T_r .

Figure 10 shows the influence of torsional rigidity T_r on the vibration of plate-type clamped-clamped end condition traversed by MDF at a constant speed. Evidently, for fixed values of elastic foundation, an increase in the torsional rigidity results in a decrease in the displacement of the plate-type structure.

Figure 11 depicts the effect of torsional rigidity, T_r on the flexural motions of plate-type clamped –ends plate-type for the MDF at a constant speed. Higher values of torsional rigidity T_r produce a decrease in the deflection profile of the structural member for the clamped-clamped boundary conditions considered. In a similar manner, an increase in the torsional rigidity of the MDM system produces a rise in the plate-type magnitude under a moving loading system at a constant speed.

The curves (12) show the effects of R_0 for the plate-type CC-ends moved by MDF at a uniform speed. Evidently, for fixed values Q_0 and T_r , an increase in the torsional rigidity results in a decrease in the displacement of the plate-type structure.

Figure 13 depicts the dynamic effect of R_0 on the flexural motions of plate-type clamped-clamped traversed by MDM at a uniform speed. Clearly, higher values of R_0 produce a decrease in the deflection profile of the structural member.

Dynamic comparability of profile for MDF and MDM plate-type at clamped ends for Q_0 & R_0 (fixed values) is given in figure 14. Clearly, the magnitude of MDM deflects at a higher rate than the MDF system at a uniform speed in the three boundary conditions considered. Figure 15 shows a comparison of Analytical and Numerical solutions of the plate-type lying on the variable elastic subgrade.

Table 1 gives the comparison analysis of MDF and MDM for the CC-ends and SC-ends for fixed values of Q_0, T_r and R_0 . From above, response of MDM is at higher rate than the MDF system.

Hence, one runs a risk of relying on the dynamic response to MDF as a better simulation to MDM of plate-type structural member.

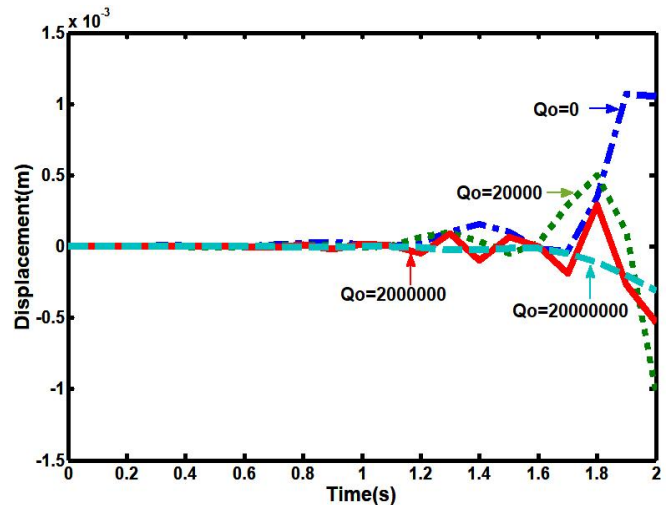


Fig. 1. Profiles of SC-ends plate-type traversed by MDF (for varying Q_0 , & fixed T_r, R_0)

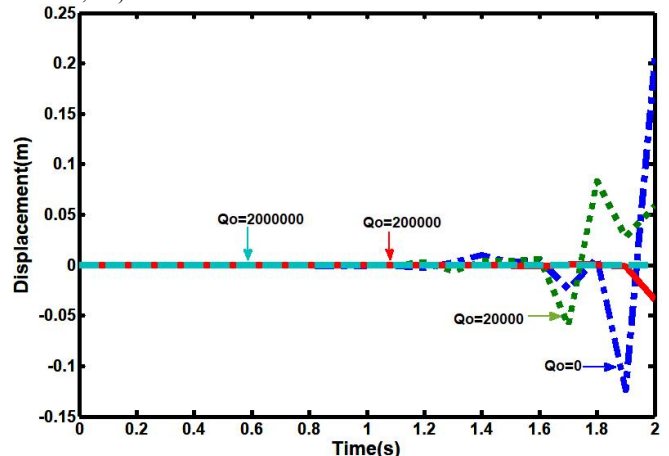


Fig. 2. Profiles of SC-ends plate-type traversed by MDM (for varying Q_0 , & fixed T_r, R_0)

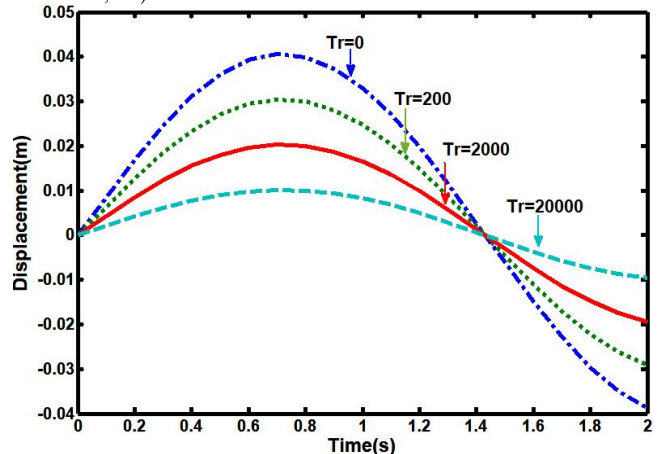


Fig. 3. Profiles of SC-ends plate-type traversed by MDF (for varying T_r & fixed Q_0, R_0)

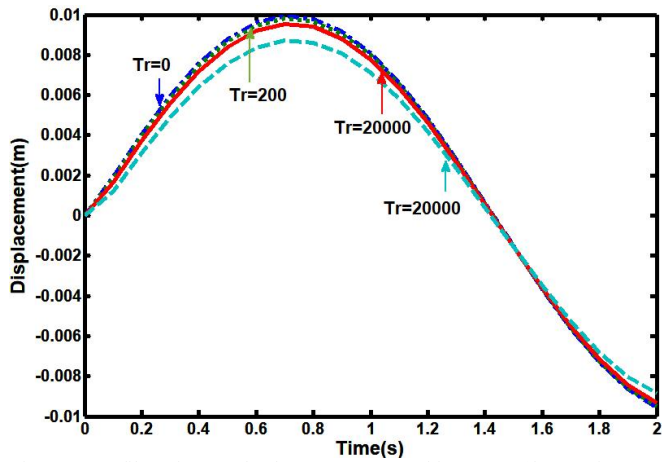


Fig. 4. Profiles of SC-ends plate-type traversed by MDM (for varying Tr & fixed Q_o, R_o)

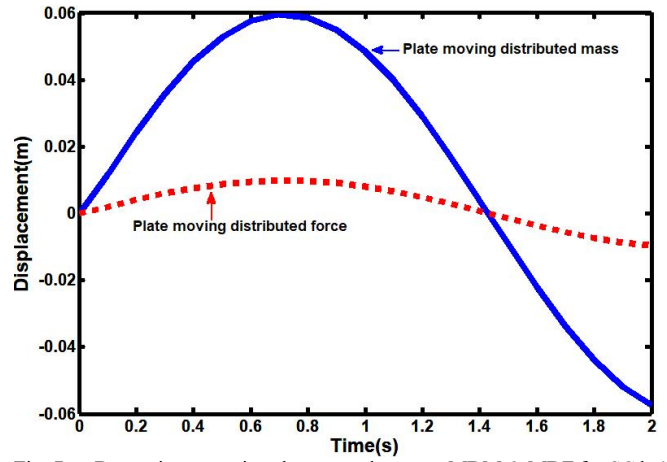


Fig. 7. Dynamic comparison between plate-type MDM & MDF for SC bc's on the variable elastic subgrade

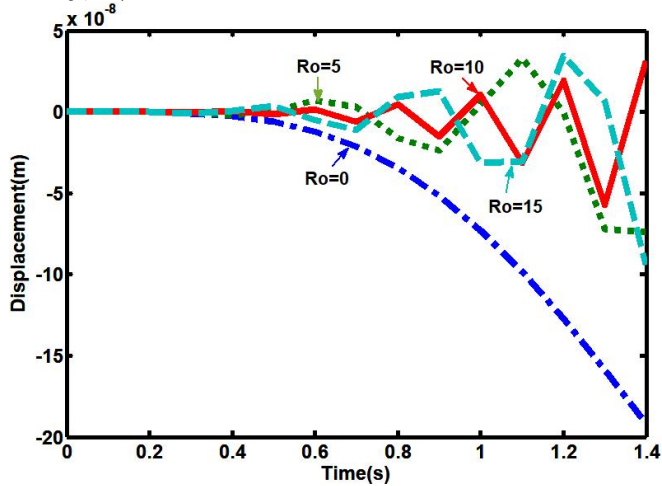


Fig. 5. Profiles of SC-ends plate-type traversed by MDF (for varying R_o & fixed Tr, Q_o)

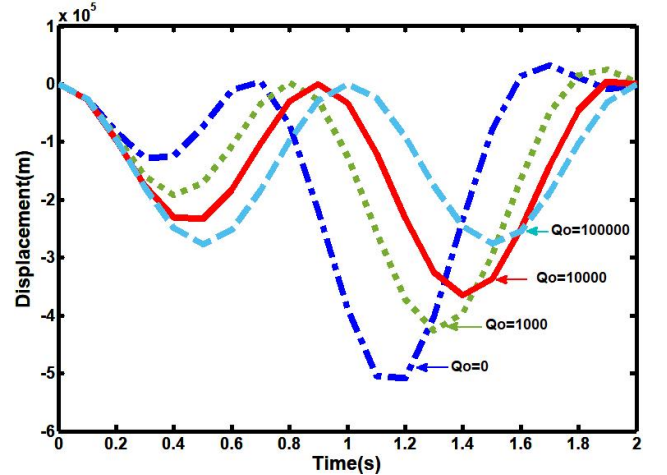


Fig. 8. Displacement profile of clamped-ends plate-type traversed by MDF (for varying Q_o & fixed Tr, R_o)

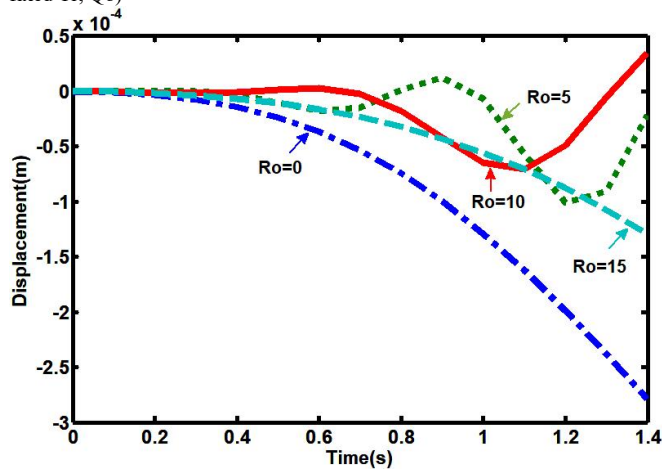


Fig. 6. Profiles of SC-ends plate-type traversed by MDF (for varying R_o & fixed Tr, Q_o)

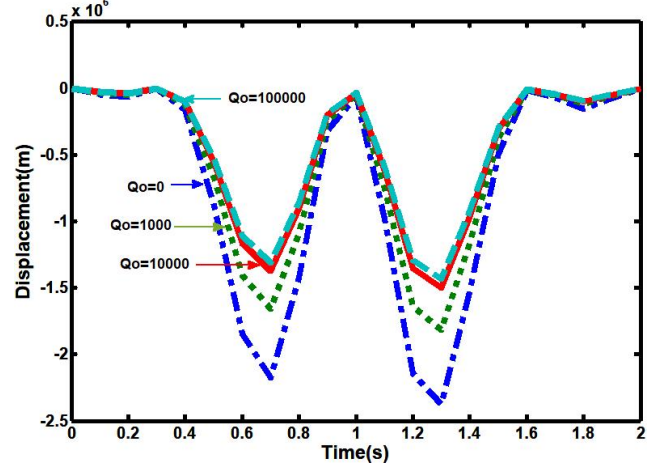


Fig. 9. Displacement profile of clamped-ends plate-type traversed by MDM (for varying Q_o & fixed Tr, R_o)

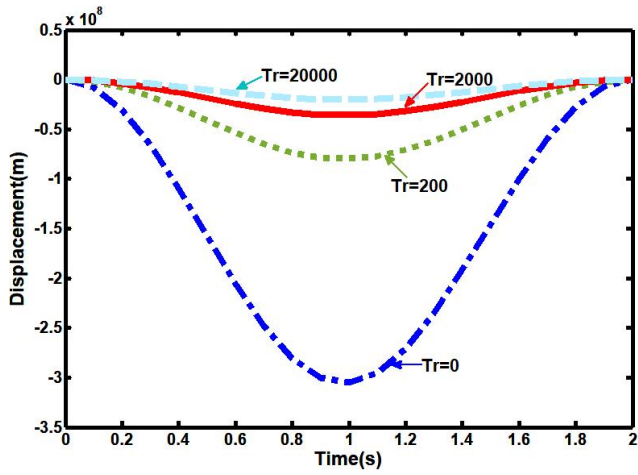


Fig. 10. Displacement profile of clamped-ends plate-type traversed by MDF (for varying T_r & fixed Q_o, R_o)

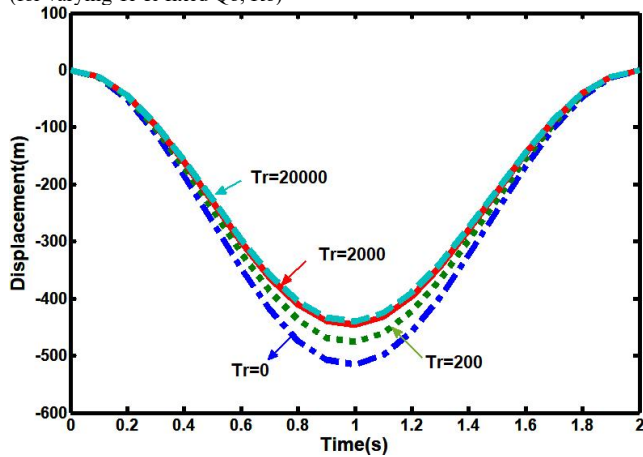


Fig. 11. Displacement profile of clamped-ends plate-type traversed by MDM (for varying T_r & fixed Q_o, R_o)

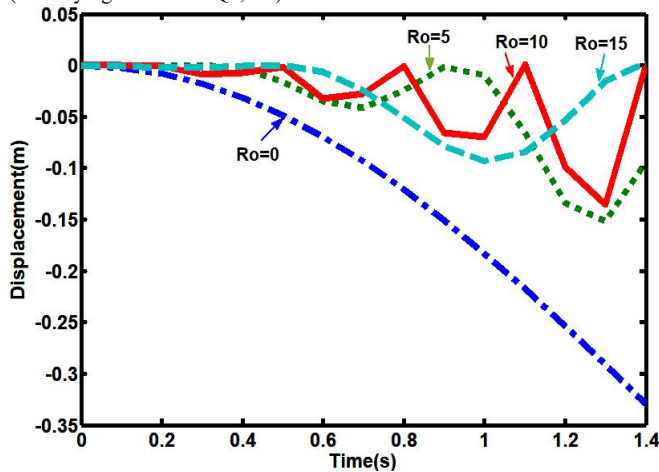


Fig. 12. Displacement profile of clamped-ends plate-type traversed by MDF (for varying R_o & fixed T_r, Q_o)

VII. CONCLUSION

This paper considers an assessment of the displacement response of plate-type simple-clamped and clamped-clamped ends conditions at uniform velocity. Analytical procedures for the model equation are achieved by the separation of variable methods to obtain a dynamic solution for MDF and MDM problems. From the analyzed solution, the condition under which the resonance occurs has been established and therefore noted that the speed (critical) of the plate-type moved by

MDM is of smaller magnitude compared to the plate-type traversed by

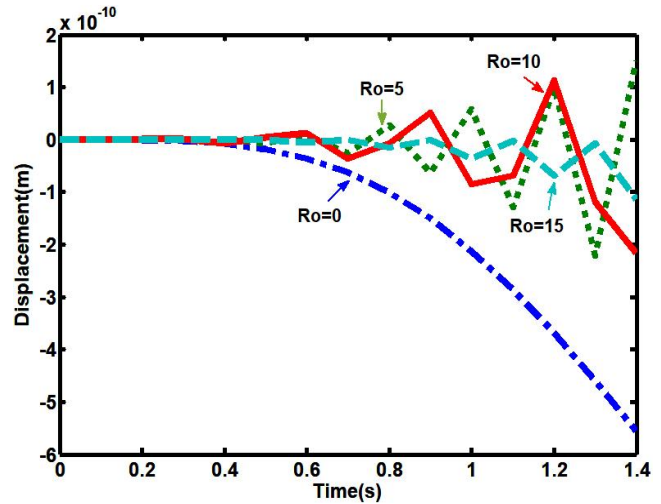


Fig. 13. Displacement profile of clamped ends plate-type traversed by MDM (for varying R_o & fixed T_r, Q_o)

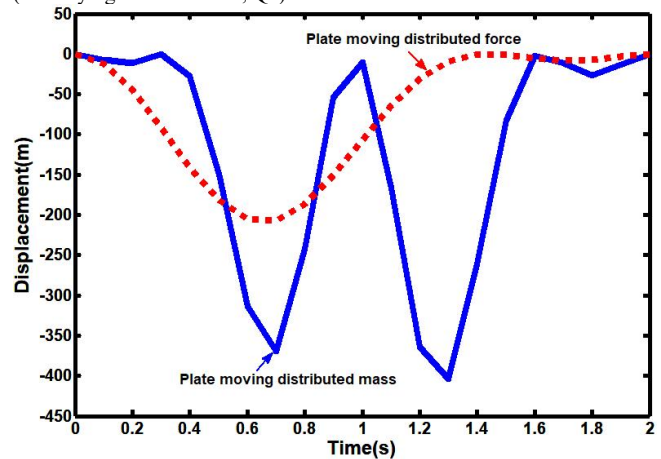


Fig. 14. Dynamic comparison between plate-type MDM & MDF for Clamped-ends bc's on the variable elastic subgrade

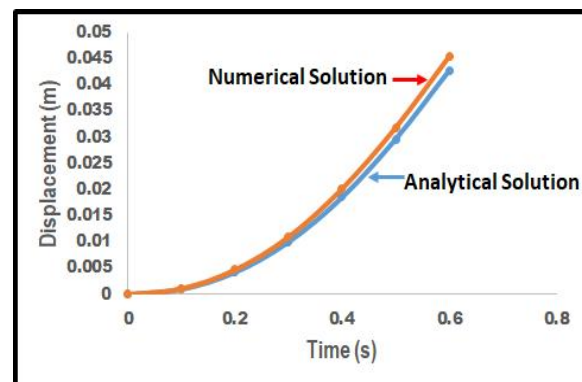


Fig. 15. Comparison of Numerical & Analytical procedural solutions of plate-type lying on variable elastic subgrade

MDM with the same natural frequency. Also, it is evident that resonance condition is previously attained in MDM than in the MDF system. It is noted that the technique employed in this paper yields solutions to any desired degree of accuracy. Finally, there is an excellent agreement between the results presented in this study and the existing results.

TABLE 1

Comparison of Analytical and Numerical solutions of the plate-type lying on variable elastic subgrade

S/N	T(sec.)	MDF	MDM
1	0	4.71E-04	3.76E-06
2	0.1	2.64E-03	1.06E-04
3	0.2	3.08E-03	1.20E-04
4	0.3	1.42E-03	7.34E-05
5	0.4	-1.23E-03	7.80E-06
6	0.5	-3.42E-03	-4.94E-05
7	0.6	-4.43E-03	-1.28E-04
8	0.7	-4.37E-03	-2.35E-04
9	0.8	-3.71E-03	-3.14E-04
10	0.9	-2.79E-03	-2.95E-04
11	1	-1.70E-03	-1.65E-04
12	1.1	-4.20E-04	-1.22E-05
13	1.2	9.94E-04	1.61E-04
14	1.3	2.24E-03	2.51E-04
15	1.4	2.82E-03	3.03E-04
16	1.5	2.45E-03	3.34E-04
17	1.6	1.32E-03	2.88E-04
18	1.7	7.29E-05	1.78E-04
19	1.8	-7.10E-04	2.98E-05
20	1.9	-8.97E-04	-8.19E-05

REFERENCES

[1] L. Fryba, *Vibration of solids and structures under moving loads*. Groningen: Noordhoff, 1972.
 [2] S. T. Oni, "Human Safety: Complexity of response of Structural members when under moving loads' Inaugural Lecture series 47, the Federal University of Technology, Akure, Nigeria, 2007.
 [3] M. Milormir, M. M. Stanasic, and J. C. Hardin, "On the response of beam to an arbitrary number of concentrated moving masses," *Journal of Franklin Institute*, vol. 287, no. 2, 1969.
 [4] S. N. Ogunyebi, A. Adedowole, T. O. Ogunlade, and A. A. Oyedele, "Flexural Motions of Beams on Foundation Subjected to Moving Concentrated Force", *International Journal of Engineering and Advanced Technology (IJEAT)*, vol. 9, no. 3, pp. 2249–8958, 2020. DOI: 10.35940/ijeat.C5691.029320
 [5] M. S. Al-Ansari and M. S. Afzal, "Regular and Irregular Plate Deflection Analysis using Matrix Method", *IOSR Journal of Mechanical and Civil Engineering*, vol. 16, (1) Ser. IV, pp. 24-40, 2019. DOI: 10.9790/1684-1601042440
 [6] V. N. Fedoseyeva and D. A. Yagnyatinskiya, "Deflection of a Thin Rectangular Plate with Free Edges under Concentrated Loads", *Mechanics of Solids*, vol. 54, no.5, pp. 750–755, 2019.

[7] T. Gebre, V. Galishnikova and E. Tupikova, "Warping Behavior of Open and Closed Thin-Walled Sections with Restrained Torsion," *Engineering Letters*, vol. 30, no. 1, pp. 354-361, 2022.
 [8] S. N. Ogunyebi, "Dynamic Influences of Constant and Variable Elastic Foundations on Elastic Beam under Exponentially Varying Magnitude Moving Load", *International Journal of Scientific and Research Publications*, vol.10, no. 6, pp. 997-1003, 2020. DOI: 10.29322/IJSRP.10.06.2020.p102120.
 [9] E. Esmailzadeh, and M. Gorashi, "Vibration of beams traversed by uniform partially distributed moving masses", *Journal of Sound and Vibration*, vol. 184, pp. 9-17, 1995.
 [10] S. Wu, M. L. Lee and T. S. Lai, "The Dynamic analysis of a flat plate under a moving load by the Finite Element Method", *International Journal of Numerical Methods in Engineering*, vol. 24, pp. 743-762, 1987.
 [11] S. T. Oni and S. N. Ogunyebi, "Dynamical Analysis of finite prestressed Bernoulli- Euler beams with general boundary conditions under traveling distributed loads", *Journal of the Nigerian Association of Mathematical Physics*, vol. 12, pp. 87-102, 2008.
 [12] S. T. Oni and S. N. Ogunyebi, "Dynamic Response of Uniform Rayleigh Beams on Variable Bi-parametric Elastic Foundation under Partially Distributed Loads", *Asian Journal of Applied Science*, vol. 11, 10.3923/ajaps.2018.199-212.
 [13] J. Gao, F. Dang, Z. Ma, and J. Ren, "Deformation and Mechanical Behaviors of SCSF and CCCF Rectangular Thin Plates Loaded by Hydrostatic Pressure," *Advances in Civil Engineering*, vol. 2019, pp. 1-12, 2019. <https://doi.org/10.1155/2019/1560171>
 [14] S. Sorrentino and G. Catania, "Dynamic analysis of rectangular plates crossed by distributed moving loads," *Mathematics and Mechanics of Solids*, vol. 23, no. 9, pp. 1291-1302, 2018. <https://doi.org/10.1177/1081286517719120>
 [15] S. W. Alisjahbana, S. Sumawiganda, and S. Leman, "Dynamic of rigid roadway pavement under dynamic loads," 34th Conference on our world in concrete and structures. Singapore, 2009. <http://cipremier.com/100034006>
 [16] M. R. Shadnam, M. Mofid, and J. E. Akin, "On the dynamic response of rectangular plate with moving mass," *Thin-walled Structures*, vol. 39. pp. 797-806, 2001.

Date of modification: 15th July, 2023.

Brief description of the change: add back reference citations ([3] to [14]) in the paper content.